

Symmetric Stereographic Orientation Parameters Applied to Constrained Spacecraft Attitude Control

Charles M. Southward II , Joshua R. Ellis , and Hanspeter Schaub

Simulated Reprint from

Journal of the Astronautical Sciences

Vol. 55, No. 3, July–Sept., 2007, Pages 389-405

A publication of the
American Astronautical Society
AAS Publications Office
P.O. Box 28130
San Diego, CA 92198

Symmetric Stereographic Orientation Parameters Applied to Constrained Spacecraft Attitude Control*

Charles M. Southward II[†], Joshua R. Ellis[‡], and Hanspeter Schaub[§]

Abstract

The full kinematic properties of a minimal set of rigid body attitude coordinates called Symmetric Stereographic Orientation Parameters (SSOPs) are developed. These coordinates result from a stereographic projection of the Euler parameter constraint hypersphere onto a three-dimensional hyper-plane. As discussed in previous work,⁵ this family contains the well known classical and modified Rodrigues parameters. Considering general SSOP projection points, transformations to the Euler parameters and the direction cosine matrix are discussed. The set of three SSOP coordinates have the unique feature that the associated singularity can be placed at a desired principal rotation angle by adjusting the projection point. In contrast to the Rodrigues parameters, the SSOP coordinates do not represent a unique orientation. The impact of this non-uniqueness on the constrained spacecraft attitude control problem is discussed. An attitude feedback control law in terms of SSOPs will inherently avoid reaching this singular attitude description, and thus constrain the attitude error response to be within a well defined cone. Lyapunov's direct method is used to illustrate how a SSOP-based control law can be derived to drive the spacecraft attitude away from the singularity and towards a desired orientation. This control law generalizes the previously developed classical and modified Rodrigues parameter based attitude control laws for general stereographic projection points.

1 Introduction

The study of rigid body attitude representations is both an old and continuing field of study that has drawn the attention of some of the greatest scholars of classical mechanics. Many have sought to devise the "perfect" rigid body attitude representation in spite of the fact that several roadblocks stand firmly in the path toward this goal. In particular, one must use at least three independent parameters to describe the general attitude of a rigid body, and any such minimal representation will always have an associated mathematical singularity.¹ This singularity can be eliminated by introducing additional, and thus redundant, coordinates into an attitude representation; however, doing so can increase the complexity of the representation and inevitably introduces constraints that must be satisfied at all times.

*17th AAS/AIAA Space Flight Mechanics Meeting, Sedona, Arizona, Jan. 28 - Feb. 1, 2007

[†]Graduate Student, Aerospace and Ocean Engineering Department, Virginia Tech.

[‡]Graduate Student, Aerospace and Ocean Engineering, Virginia Tech, National Defense Science and Engineering Graduate Fellow.

[§]Assistant Professor, Aerospace and Ocean Engineering Department, Virginia Polytechnic Institute, Senior AIAA Member.

In 1962, Wiener discussed the modified Rodrigues parameters (MRPs) in his doctoral thesis, though they were not called by this name at the time. Compared to the classical Rodrigues parameters (CRPs), MRPs have the interesting property that they only become singular for 360° principal rotations. Marandi and Modi discuss the numerical advantages of the MRPs in Reference 2. In 1993, Shuster discussed the basic kinematic properties of the MRPs in his extensive survey of attitude representations.³ Tsiotras in Reference 4 presents an elegant linear control law in terms of MRPs and shows nonlinear stability of the resulting closed-loop attitude motion. Further, Tsiotras mentions in this paper that the MRPs can be viewed as a stereographic projection of the Euler parameter unit constraint sphere onto a three-dimensional hyper-plane. This concept of using a stereographic projection to reduce the four-dimensional Euler parameters to a minimal attitude coordinate set was expanded by Schaub and Junkins in Reference 5 to develop a family of minimal attitude coordinates called the Symmetric and Asymmetric Stereographic Orientation Parameters (SSOPs and ASOPs). In particular, this paper shows that the SSOPs contain both the CRPs and MRPs, in that the CRPs and MRPs are obtained by placing the projection point at either $\beta_0 = 0$ or $\beta_0 = -1$. The MRP shadow set properties are also explored. Reference 5 presents how the kinematic properties of the general SSOP can be obtained, but does not provide any analytical results.

An interesting property of the SSOPs is that the principal rotation angle at which the attitude representation is singular can be freely chosen. This has interesting implications for attitude control law developments, where a “singularity cone” can be created about the reference attitude as illustrated in Fig. 1. This paper fully develops the general kinematic properties of the SSOP by providing analytical expressions for the mapping from SSOP to the direction cosine matrix, as well as the differential kinematic expressions. All results are in terms of a stereographic projection point location. Further, duality issues of the SSOPs are carefully examined. For a given attitude there are two corresponding distinct sets of MRPs, and similarly for a given set of MRPs there is no ambiguity regarding the actual spacecraft attitude. However, with the general SSOPs, the mapping from attitude coordinates to spacecraft orientation is not necessarily unique and must be addressed.

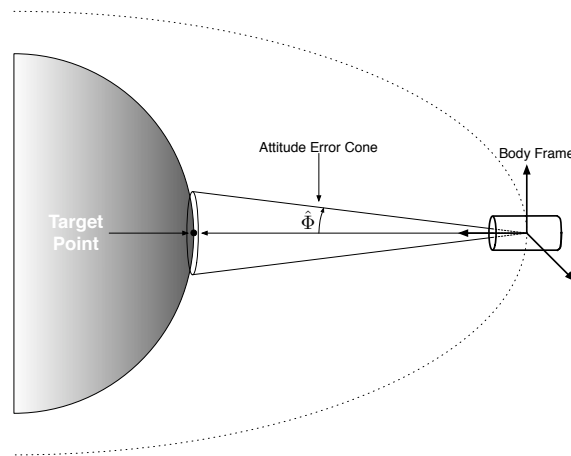


Figure 1. Illustration of Spacecraft Pointing Accuracy Requirement.

Spacecraft attitude control is a subject that has been studied at length in the literature. In light of the SSOP discussion presented above, an attitude control law that tracks a reference trajectory while never deviating from the reference by more than a specified amount is one example of the usefulness of the SSOPs. Akella⁶ develops an attitude control law based on the modified Rodrigues parameters that drives the attitude to a desired orientation without the need for angular velocity feedback. However, this control law allows the spacecraft to rotate through any attitude as it is brought to the desired orientation. Spindler⁷ studied a similar situation by considering rest-to-rest rigid body attitude maneuvers that avoid a certain “forbidden” direction. A cost function is

developed that penalizes high angular velocities as well as close proximity to the forbidden direction, and linear optimal control techniques are used to minimize the cost function and determine a suitable control law. This method could be adapted to bound the attitude of a spacecraft around a desired orientation, but it would require the introduction of multiple, if not infinite, forbidden directions.

An SSOP-based control method is presented as a potential application of the SSOPs to bound the attitude error motion of a rigid body without considering torque limitation constraints. This simple method does not require the use of multiple cost functions to penalize deviations from the reference trajectory, as the “penalty” is directly built into the attitude coordinates. On the singularity cone the SSOPs are infinite. Thus, by placing the singularity cone at the tolerance angle with which we would like to regulate a spacecraft’s attitude, simple feedback control laws are designed in which the control torque grows unbounded as the spacecraft attitude approaches the tolerance angle. In this way, the attitude motion around the reference trajectory is bounded using the inherent properties of the attitude coordinates. This avoids the need for cost functions or other devices that penalize deviation from a reference orientation. Note that the resulting control laws generalize previously developed MRP and CRP attitude control laws^{5,8} for arbitrary projection points. The analytical stability and feedback gain discussions reduce to the CRP and MRP solutions for their respective projection points. If such SSOP based attitude control laws were employed for the constrained pointing control problem, then saturated torque issues and sensing accuracy issues would need to be addressed. With control torque limitations, global stability without violating the constraint placed on the SSOPs to resolve the duality issue is no longer possible. Instead, methods using Lyapunov optimal control techniques⁹ could be used, or the saturated control strategy by Wallsgrove and Akella¹⁰ could be adapted for use with the SSOPs.

The remainder of this paper is organized as follows. In Section 2, the general SSOP kinematic relationships are developed for arbitrary stereographic projection points on the scalar Euler parameter β_0 axis. In particular, the analytical direction cosine matrix and the kinematic differential equations for the SSOPs are derived. Also, the duality issue in the definition of the general SSOPs, which was not addressed in Reference 5, is presented in this paper. Two attitude control laws based on the SSOPs that generalize previously developed CRP and MRP control laws for general projection points are developed in Section 3. Analytical expressions for feedback gain selections using the linearized closed loop dynamics are presented. Numerical simulations are presented to illustrate how the control laws bound the attitude motion about the reference orientation.

2 Symmetric Stereographic Orientation Parameters

While Reference [5] presents the concept of symmetric stereographic orientation parameters, only the basic definition of the SSOP is discussed. This section fully develops the kinematics of the SSOPs and discusses the uniqueness of the orientation represented by a particular set of SSOPs, $\boldsymbol{\eta}$.

2.1 Generalized Attitude Coordinates

Tsiotras shows in Reference [11] that the MRPs¹² can be obtained through a stereographic projection of the Euler parameter unit constraint hypersphere onto a three-dimension projection plane. This technique allows us to map the four dimensional Euler parameters, which are constrained to the surface of a unit hypersphere, onto a three dimensional surface. In a later work, Schaub and Junkins demonstrated that the MRPs and the CRPs are in fact members of a larger class of attitude coordinates called the Symmetric Stereographic Orientation Parameters (SSOPs).⁵

Figure 2 depicts a two-dimensional representation of the four dimensional Euler parameter unit constraint surface (S). The Euler parameters are given by the coordinates $\{\beta_0, \beta_1, \beta_2, \beta_3\}$ where β_0 is the scalar term. The figure also shows the projection point (A) on the β_0 axis which is a distance a from the origin. The positioning of A dictates where the SSOPs become singular. The SSOP Hyperplane (P) is placed a unit distance to the right of A . A line drawn from A to the Euler parameters on S passes through P ; the point it passes through is the SSOP which is denote as $\boldsymbol{\eta} = [\eta_1 \ \eta_2 \ \eta_3]^T$. Notice as the Euler parameters ($\boldsymbol{\beta}$) approach the value directly above A , the

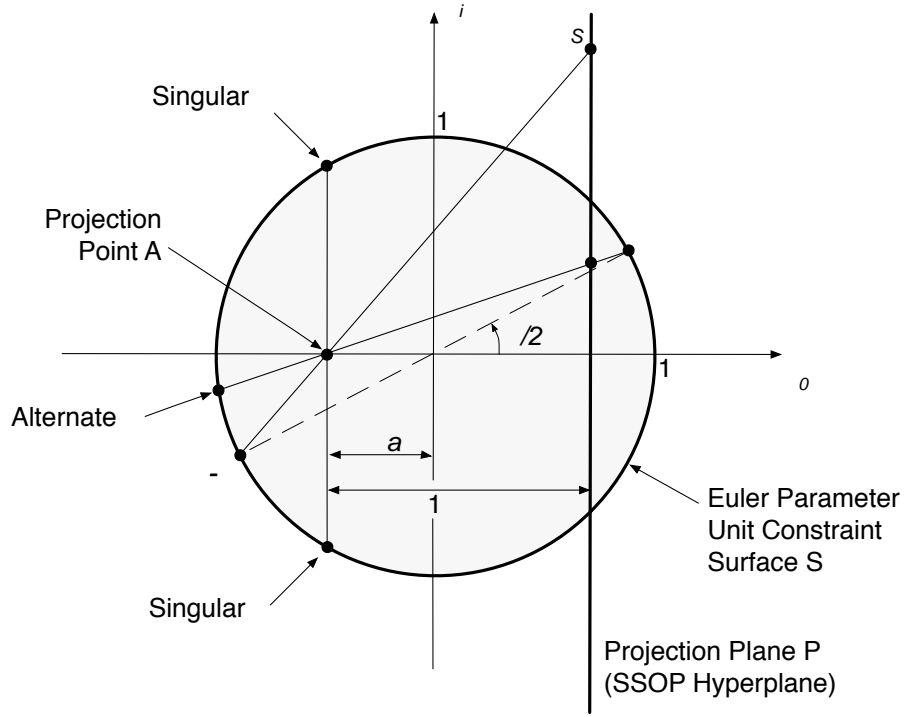


Figure 2. Two-Dimensional Representation of the Stereographic Projection of the Euler Parameter Unit Constraint Sphere Onto the SSOP Three-Dimensional Hyperplane.

values of η grow toward infinity creating a singularity, a fact that is exploited in the control law development. By means of simple geometry and algebra, η can be written in terms of the Euler parameters and the variable a as follows:⁵

$$\eta_i = \frac{\beta_i}{\beta_0 - a} \quad i = 1, 2, 3 \quad (1)$$

Studying equation (1), it is evident that there is a singularity when $a = \beta_0$. The parameter β_0 is related to the principal rotation angle by

$$\beta_0 = \cos\left(\frac{\Phi}{2}\right) \quad (2)$$

Using this relation, a value for a is selected such that the SSOPs become singular at a desired principal rotation angle. This singularity is beneficial when trying to control a spacecraft with a finite pointing error because a SSOP-based feedback employs infinite torque commands to keep the spacecraft from penetrating this allowable pointing error cone.

Next, the inverse mapping from SSOPs to Euler parameters is determined. Combining the Euler parameter unit constraint with equation (1), the following quadratic form in terms of β_0 is obtained:

$$(1 + \boldsymbol{\eta}^T \boldsymbol{\eta}) \beta_0^2 - 2a\boldsymbol{\eta}^T \boldsymbol{\eta} \beta_0 + a^2 \boldsymbol{\eta}^T \boldsymbol{\eta} - 1 = 0 \quad (3)$$

This equation is solved to yield the following inverse-transformation

$$\beta_0 = \frac{a\eta^2 \pm \sqrt{1 + (1 - a^2)\eta^2}}{1 + \eta^2} \quad (4)$$

where the shorthand notation $\eta^2 = \boldsymbol{\eta}^T \boldsymbol{\eta}$ is used. Equation (4) shows that there is a duality associated with the SSOPs, in that a given $\boldsymbol{\eta}$ can describe two distinctly different attitudes. This duality is illustrated in Fig. 2 with the two possible attitudes labeled as “ $\boldsymbol{\beta}$ ” and “alternate $\boldsymbol{\beta}$.” Because of the position of A along the β_0 axis, both of these points on S are projected through A onto the same point on P . Thus, given a set of SSOPs without any other knowledge of the motion, the attitude of the body in question cannot be uniquely determined. However, note that there are three special classes of SSOPs for which this duality does not exist: SSOPs with $a = 0$ (CRPs), $a = -1$ (MRPs), and $a = 1$. For $a = 0$, the projection point is the center of S , so the two possible attitudes are in fact identical ($\boldsymbol{\beta}$ and $-\boldsymbol{\beta}$)—a fact that can easily be derived from equation (4). For $a = \pm 1$, one of the possible attitudes is fixed at $\beta_0 = \pm 1$, while the other is free to change on S ; however, the fixed attitude is located at the associated mathematical singularity, and is therefore unattainable. As a result, the body must always have the attitude that is free on S , and the duality is eliminated.

For SSOPs with $a \neq 0, \pm 1$, a method must be devised that eliminates the duality described above. One possibility is to use another piece of information, such as the principal rotation angle, that would allow for the exact determination of the attitude. Another possibility that requires no additional information is to constrain the definition of the SSOPs such that there is only one possible attitude for a given $\boldsymbol{\eta}$. Studying Fig. 2, notice that constraining the definition of the SSOPs to $\beta_0 > a$ or $\beta_0 < a$ eliminates the duality. Combining this constraint with equation (4), the following is obtained:

$$\beta_0 = \frac{a\eta^2 + \sqrt{1 + (1 - a^2)\eta^2}}{1 + \eta^2} \implies \beta_0 > a \quad (5a)$$

$$\beta_0 = \frac{a\eta^2 - \sqrt{1 + (1 - a^2)\eta^2}}{1 + \eta^2} \implies \beta_0 < a \quad (5b)$$

These results can be easily proven by considering the inequalities $\sqrt{1 + (1 - a^2)\eta^2} > a$ and $\sqrt{1 + (1 - a^2)\eta^2} > -a$ for $a \in [-1, 1)$ and performing some simple algebraic manipulations. Thus, if a set of SSOPs is desired to describe attitudes with $\beta_0 > a$, equation (5a) must be used as the inverse transformation from SSOPs to Euler parameters. Conversely, equation (5b) must be used to obtain attitudes with $\beta_0 < a$. In the remainder of this paper, it is assumed that attitudes with $\beta_0 > a$ are desired and derive all subsequent results accordingly. If one desires attitudes with $\beta_0 < a$, the derivations presented in the rest of the paper can be followed step by step using equation (5b) in place of equation (5a). The reason for this assumption is that $\beta_0 > 0$ is ideal for the attitude pointing problem, in which the attitude tracking errors need to be bounded within a specified principal rotation angle $\hat{\Phi} < \pi$. For this application the duality issues have no practical effect.

To simplify equations (5a) and (5b), let us define the Σ_i parameters as

$$\Sigma_1 = a\eta^2 + \sqrt{1 + \eta^2(1 - a^2)} \quad (6)$$

$$\Sigma_2 = -a + \sqrt{1 + \eta^2(1 - a^2)} \quad (7)$$

For the case where $\beta_0 > 0$, this yields simpler transformations from the SSOP coordinates to the Euler parameters:

$$\beta_0 = \frac{\Sigma_1}{1 + \eta^2} \quad (8)$$

$$\beta_i = \eta_i \frac{\Sigma_2}{1 + \eta^2} \quad (9)$$

Note that the two Σ_i terms are not constants, but rather functions of the SSOP coordinates. Taking $a \in [-1, 1)$, it must be true that $1 - a^2 \geq 0$, and therefore the radical term in equations (6) and (7) is always greater than or equal to one. Meaning Σ_1 and Σ_2 are greater than zero for any $\boldsymbol{\eta}$ and $a \in [-1, 1)$. Notice, however, that Σ_2 becomes zero when $a = 1$. A projection point at $a = 1$ corresponds to a desired singular principal rotation angle of 0° , meaning the reference attitude of the spacecraft is always at the singularity. Intuitively, this would seem to be a bad principal angle to begin with—an idea that is explored when developing the control law later in the paper.

At first glance, constraining the SSOPs to only describe specific attitudes may seem like a compelling reason *not* to choose the SSOPs for rigid body attitude error representation. This reasoning is valid if one is considering general attitude errors such as with tumbling bodies. However, the principal motivation behind the development of the general SSOPs is their application to attitude control problems with hard limits on the allowable attitude deviations. Because a set of SSOPs can be designed to become singular at any principal rotation angle, a feedback control law can be designed based on SSOPs that forces a body to never deviate from a reference state beyond this singular principal rotation angle. As this singular principal rotation angle is essentially the dividing line between the attitudes chosen to describe the SSOPs and those attitudes for which there is no description, the duality of the SSOPs is not a problem as long as they are used in the proper setting.

2.2 Direction Cosine Matrix

The Direction Cosine Matrix, or DCM, is parameterized in terms of the general SSOPs by first considering the parameterization of the DCM in terms of Euler parameters:¹

$$[C] = \begin{bmatrix} \beta_0^2 + \beta_1^2 - \beta_2^2 - \beta_3^2 & 2(\beta_1\beta_2 + \beta_0\beta_3) & 2(\beta_1\beta_3 - \beta_0\beta_2) \\ 2(\beta_1\beta_2 - \beta_0\beta_3) & \beta_0^2 - \beta_1^2 + \beta_2^2 - \beta_3^2 & 2(\beta_2\beta_3 + \beta_0\beta_1) \\ 2(\beta_1\beta_3 + \beta_0\beta_2) & 2(\beta_2\beta_3 - \beta_0\beta_1) & \beta_0^2 - \beta_1^2 - \beta_2^2 + \beta_3^2 \end{bmatrix} \quad (10)$$

Substituting equations (8) and (9) into equation (10) and recalling the definitions of the parameters Σ_1 and Σ_2 , the following parameterization is obtained:

$$[C] = \frac{1}{(1 + \eta^2)^2} \begin{bmatrix} [\Sigma_1^2 + (\eta_1^2 - \eta_2^2 - \eta_3^2) \Sigma_2^2] & 2[\eta_1\eta_2\Sigma_2^2 + \eta_3\Sigma_1\Sigma_2] & 2[\eta_1\eta_3\Sigma_2^2 - \eta_2\Sigma_1\Sigma_2] \\ 2[\eta_1\eta_2\Sigma_2^2 - \eta_3\Sigma_1\Sigma_2] & [\Sigma_1^2 + (-\eta_1^2 + \eta_2^2 - \eta_3^2) \Sigma_2^2] & 2[\eta_2\eta_3\Sigma_2^2 + \eta_1\Sigma_1\Sigma_2] \\ 2[\eta_1\eta_3\Sigma_2^2 + \eta_2\Sigma_1\Sigma_2] & 2[\eta_2\eta_3\Sigma_2^2 - \eta_1\Sigma_1\Sigma_2] & [\Sigma_1^2 + (-\eta_1^2 - \eta_2^2 + \eta_3^2) \Sigma_2^2] \end{bmatrix} \quad (11)$$

Equation (11) can also be written in a compact matrix form as follows:

$$[C] = \frac{1}{(1 + \eta^2)^2} \left[\Sigma_2^2 \left([\tilde{\eta}]^2 + \boldsymbol{\eta}\boldsymbol{\eta}^T \right) - 2[\tilde{\eta}] \Sigma_1 \Sigma_2 + \Sigma_1^2 [I]_{3 \times 3} \right] \quad (12)$$

where $[\tilde{\eta}]$ is the skew symmetric matrix with components of $\boldsymbol{\eta}$.

Note that this DCM parameterization reduces to the MRP and CRP parameterizations for $a = -1$ or $a = 0$, respectively. There is no convenient direct transformation to perform the inverse mapping from the DCM to $\boldsymbol{\eta}$ parameters. Instead the DCM is first converted to Euler parameters using Stanley's method,¹³ and then converted to the general SSOPs using equation (1).

2.3 Kinematic Differential Equations

The kinematic differential equations of the SSOPs are derived in an analogous manner to the DCM by first considering the kinematic differential equations of the Euler parameters:

$$\begin{pmatrix} \dot{\beta}_0 \\ \dot{\beta}_1 \\ \dot{\beta}_2 \\ \dot{\beta}_3 \end{pmatrix} = \frac{1}{2} \begin{bmatrix} \beta_0 & -\beta_1 & -\beta_2 & -\beta_3 \\ \beta_1 & \beta_0 & -\beta_3 & \beta_2 \\ \beta_2 & \beta_3 & \beta_0 & -\beta_1 \\ \beta_3 & -\beta_2 & \beta_1 & \beta_0 \end{bmatrix} \begin{pmatrix} 0 \\ \omega_1 \\ \omega_2 \\ \omega_3 \end{pmatrix} \quad (13)$$

Equation (1) is differentiated to give

$$\dot{\boldsymbol{\eta}} = \frac{(\beta_0 - a)\dot{\boldsymbol{\beta}}_i - \boldsymbol{\beta}_i\dot{\beta}_0}{(\beta_0 - a)^2} \quad (14)$$

where $\boldsymbol{\beta}_i = [\beta_1 \ \beta_2 \ \beta_3]^T$. The differential kinematic equations in equation (13) are substituted into equation (14) to produce the following:

$$\dot{\boldsymbol{\eta}} = \frac{1}{2} \left[\frac{\Sigma_1}{\Sigma_2} [I]_{3 \times 3} + [\tilde{\eta}] + \boldsymbol{\eta}\boldsymbol{\eta}^T \right] \boldsymbol{\omega} = \frac{1}{2} [D(\boldsymbol{\eta})] \boldsymbol{\omega} \quad (15)$$

Note that the Σ_2 value in the denominator can never be zero for any value of $\boldsymbol{\eta}$ or $a \neq 1$ as stated in the development of the SSOPs. Equation (15) can also be expanded into the following matrix form:

$$\dot{\boldsymbol{\eta}} = \frac{1}{2} \begin{bmatrix} \frac{\Sigma_1}{\Sigma_2} + \eta_1^2 & \eta_1\eta_2 - \eta_3 & \eta_1\eta_3 + \eta_2 \\ \eta_1\eta_2 + \eta_3 & \frac{\Sigma_1}{\Sigma_2} + \eta_2^2 & \eta_2\eta_3 - \eta_1 \\ \eta_1\eta_3 - \eta_2 & \eta_2\eta_3 + \eta_1 & \frac{\Sigma_1}{\Sigma_2} + \eta_3^2 \end{bmatrix} \boldsymbol{\omega} \quad (16)$$

A simple method to verify the above equations is to solve equation (15) with $a = 0$ and $a = -1$ and compare the result to the kinematic differential equations for CRPs and MRPs. Performing this simple substitution produces the exact kinematic differential equations for CRPs and MRPs, respectively.

3 Attitude Control Law

In this section, an attitude control law is developed to demonstrate a potential application of the SSOPs to bound the attitude error motion of a rigid body without considering torque limitation constraints. The resulting control laws are a direct generalization of the CRP and MRP feedback control laws discussed in References 5 and 4 for general projection points a . Lyapunov's direct method is used to derive a nonlinear control law for the nonlinear equations of motion and kinematic differential equations. The familiar Euler's equations of motion describe how a rigid body's angular velocity vector $\boldsymbol{\omega}$ changes with time subject to a control torque \mathbf{u} and external torque \mathbf{L} :

$$[I] \dot{\boldsymbol{\omega}} = -[\tilde{\boldsymbol{\omega}}] [I] \boldsymbol{\omega} + \mathbf{u} + \mathbf{L} \quad (17)$$

The 3×3 matrix $[I]$ is the symmetric, positive-definite centroidal spacecraft moment of inertia matrix and $[\tilde{\boldsymbol{\omega}}]$ is the skew-symmetric matrix of angular velocities and is a matrix representation of the vector cross product.¹ Combined, the kinetic differential equations in equation (17) and the SSOP kinematic differential equations in equation (15) provide the spacecraft equations of motion for the control development.

3.1 Candidate Lyapunov Functions

A control law is derived for two different candidate Lyapunov functions that are a variation of the kinetic and potential energy of the system. The first is the standard quadratic approach shown in equation (18), and the second is a logarithmic function similar to the one used for MRPs and CRPs in Reference [8]. Neither of these SSOP-based attitude control laws takes into account saturated torque issues or sensing accuracy. With control torque limitations, the attitude may slip past the singular attitude and into the other set of SSOPs described in the duality issue. Note that only the control is based on the SSOPs, while the actual attitude can be estimated using non-singular attitude coordinates. A saturated control could be developed based upon a Lyapunov optimal techniques,⁹ or the saturated control strategy by Wallsgrove and Akella¹⁰ could be adapted for use with the SSOPs.

3.1.1 Standard Quadratic Lyapunov Function

The standard quadratic attitude penalty function approach is considered because it allows individual gains on the attitude errors about each principal axis. Start by choosing the Lyapunov function as:

$$V(\delta\boldsymbol{\omega}, \boldsymbol{\eta}) = \frac{1}{2} \delta\boldsymbol{\omega}^T [I] \delta\boldsymbol{\omega} + \frac{1}{2} \boldsymbol{\eta}^T [K] \boldsymbol{\eta} \quad (18)$$

where $[K]$ is a symmetric, positive definite gain matrix and $[I]$ is the symmetric inertia matrix. All matrices in equation (18) are assumed to be taken with respect to the spacecraft body-fixed frame \mathcal{B} . The SSOPs, $\boldsymbol{\eta}$, measure the attitude error with respect to a reference trajectory, and the reference trajectory is determined by the reference angular velocity $\boldsymbol{\omega}_r$. The error in angular velocities is

defined as $\delta\boldsymbol{\omega} = \boldsymbol{\omega} - \boldsymbol{\omega}_r$. Note that $\boldsymbol{\omega}$ contains the components of the body angular velocity vector relative to the inertial frame, and is typically expressed in the body frame. The reference frame angular velocity components, $\boldsymbol{\omega}_r$, are also expressed relative to the inertial frame. The Lyapunov function is zero when $\boldsymbol{\eta} = \mathbf{0}$ and $\delta\boldsymbol{\omega} = \mathbf{0}$, and positive for all other values of $\boldsymbol{\eta}$ and $\delta\boldsymbol{\omega}$. Thus, it is positive-definite about the reference trajectory. The time derivative of the candidate Lyapunov function is:

$$\dot{V}(\delta\boldsymbol{\omega}, \boldsymbol{\eta}) = \delta\boldsymbol{\omega}^T [I] \delta\dot{\boldsymbol{\omega}} + \boldsymbol{\eta}^T [K] \dot{\boldsymbol{\eta}} \quad (19)$$

Note that the derivatives are being taken as seen by the body frame, so $\delta\dot{\boldsymbol{\omega}} = \frac{\text{d}}{\text{d}t}(\delta\boldsymbol{\omega})$ and $\frac{\text{d}}{\text{d}t}([I]) = 0$. The kinematic differential equation given by equation (15), using $\delta\boldsymbol{\omega}$ in place of $\boldsymbol{\omega}$, is substituted in place of $\dot{\boldsymbol{\eta}}$ and simplified to produce:

$$\dot{V}(\delta\boldsymbol{\omega}, \boldsymbol{\eta}) = \delta\boldsymbol{\omega}^T \left[[I] \delta\dot{\boldsymbol{\omega}} + [K] (1 + \eta^2) \frac{\Sigma_2 + a}{\Sigma_2} \boldsymbol{\eta} \right] \quad (20)$$

As stated in the development of the SSOPs, the value of Σ_2 is greater than zero for all $\boldsymbol{\eta}$ and $a \neq 1$. Therefore, the value of $\frac{\Sigma_2 + a}{\Sigma_2}$ is bounded for all $\boldsymbol{\eta}$ and $a \neq 1$. Notice that the exception, $a = 1$, corresponds to a singular principal rotation angle of 0° , meaning the control torque would need to be infinitely large to hold the spacecraft at that principal angle. Practically, a principal angle of 0° would be a poor design choice.

In order to make the Lyapunov rate negative definite, equation (20) is set equal to the following negative semi-definite function:

$$\dot{V}(\delta\boldsymbol{\omega}, \boldsymbol{\eta}) = -\delta\boldsymbol{\omega}^T [P] \delta\boldsymbol{\omega} \quad (21)$$

where $[P]$ is a symmetric, positive definite gain matrix. The Lyapunov rate can be set to any desired value because the equations of motion in equation (17) contain a control vector \mathbf{u} that can be prescribed. Equating equations (20) and (21) and noting that $\delta\boldsymbol{\omega}^T$ drops out of the equation, the autonomous closed-loop dynamics are found to be:

$$[I] \delta\dot{\boldsymbol{\omega}} + [K] (1 + \eta^2) \frac{\Sigma_2 + a}{\Sigma_2} \boldsymbol{\eta} + [P] \delta\boldsymbol{\omega} = 0 \quad (22)$$

Note that the closed-loop dynamics are autonomous because they do not depend *explicitly* on time. Next, equation (17) is substituted into the closed-loop dynamics to introduce the control vector into the equations. Therefore, $[I] \delta\dot{\boldsymbol{\omega}}$ must be rewritten into a useable form. The error angular velocity rates can be written as follows:

$$\delta\dot{\boldsymbol{\omega}} = \dot{\boldsymbol{\omega}} - \dot{\boldsymbol{\omega}}_r + [\tilde{\omega}] \boldsymbol{\omega}_r \quad (23)$$

This equation is substituted into equation (22) to obtain the following:

$$[I] \dot{\boldsymbol{\omega}} - [I] (\dot{\boldsymbol{\omega}}_r - [\tilde{\omega}] \boldsymbol{\omega}_r) + [K] (1 + \eta^2) \frac{\Sigma_2 + a}{\Sigma_2} \boldsymbol{\eta} + [P] \delta\boldsymbol{\omega} = 0 \quad (24)$$

Inserting equation (17), the components of the control vector are solved for as:

$$\mathbf{u} = [\tilde{\omega}] [I] \boldsymbol{\omega} + [I] (\dot{\boldsymbol{\omega}}_r - [\tilde{\omega}] \boldsymbol{\omega}_r) - [K] (1 + \eta^2) \frac{\Sigma_2 + a}{\Sigma_2} \boldsymbol{\eta} - [P] \delta\boldsymbol{\omega} - \mathbf{L} \quad (25)$$

Note that this feedback law is not linear in terms of the attitude error $\boldsymbol{\eta}$, but rather contains generally quartic polynomial terms. However, the attitude feedback gain is set through the matrix $[K]$, which allows the response about different axes to be set individually. To numerically evaluate the control \mathbf{u} , all angular velocity vectors components must be expressed in the body frame.

The $[\tilde{\omega}] [I] \boldsymbol{\omega}$ term in equation (25) can be replaced with $[\tilde{\omega}] [I] \boldsymbol{\omega}_r$ without influencing the stability argument. This removes the quadratic dependency on $\boldsymbol{\omega}$ which is beneficial with large initial $\boldsymbol{\omega}$ errors. However, such a control will lead to non-autonomous closed-loop equations which complicate the feedback gain selection process. The remainder of this paper uses the control torque expression in equation (25) because it provides autonomous closed-loop equations and a feedback gain selection strategy which generalizes the MRP feedback gain selection technique discussed in Reference 5.

3.1.2 Logarithmic Lyapunov Function

The standard quadratic Lyapunov function produces a term $(1 + \eta^2)$ that leads to increased nonlinearity in the control law. The logarithmic Lyapunov function is chosen to try to avoid this nonlinear scaling term. The logarithmic Lyapunov function is given as:

$$V(\delta\boldsymbol{\omega}, \boldsymbol{\eta}) = \frac{1}{2} \delta\boldsymbol{\omega}^T [I] \delta\boldsymbol{\omega} + K \ln(1 + \boldsymbol{\eta}^T \boldsymbol{\eta}) \quad (26)$$

where K is now a scalar feedback gain and $[I]$ is the inertia matrix. For the special case that the SSOPs are either MRPs or CRPs, this Lyapunov function is known to lead to a feedback which is linear in the attitude error measure.^{4,5} The time derivative of the Lyapunov function is:

$$\dot{V}(\delta\boldsymbol{\omega}, \boldsymbol{\eta}) = \delta\boldsymbol{\omega}^T \left[[I] \delta\dot{\boldsymbol{\omega}} + K \frac{\Sigma_2 + a}{\Sigma_2} \boldsymbol{\eta} \right] \quad (27)$$

As shown for the quadratic Lyapunov function, the value of $\frac{\Sigma_2 + a}{\Sigma_2}$ is bounded for all $\boldsymbol{\eta}$ and $a \neq 1$. Also notice that the nonlinear scaling term does not appear as it did for the quadratic Lyapunov function.

In order to make the Lyapunov rate negative semi-definite, equation (27) is set equal to equation (21) and noting that $\delta\boldsymbol{\omega}^T$ drops out of the equation, the autonomous closed loop dynamics are found to be:

$$[I] \delta\dot{\boldsymbol{\omega}} + K \frac{\Sigma_2 + a}{\Sigma_2} \boldsymbol{\eta} + [P] \delta\boldsymbol{\omega} = 0 \quad (28)$$

Again, equation (17) is substituted into the closed loop dynamics to introduce the control vector into the equations, and the components of the control vector are found as:

$$\mathbf{u} = [\tilde{\boldsymbol{\omega}}] [I] \boldsymbol{\omega} + [I] (\dot{\boldsymbol{\omega}}_r - [\tilde{\boldsymbol{\omega}}] \boldsymbol{\omega}_r) - K \frac{\Sigma_2 + a}{\Sigma_2} \boldsymbol{\eta} - [P] \delta\boldsymbol{\omega} - \mathbf{L} \quad (29)$$

For the special case of MRPs with $a = -1$ or CRPs with $a = 0$, the standard feedback laws discussed in References 4 and 5 are regained. However, for general SSOP coordinates the feedback law is nonlinear in terms of $\boldsymbol{\eta}$ because of the first order dependence of Σ_2 on η_i .

3.2 Asymptotic Stability Proof

Because \dot{V} is negative semi-definite for both candidate Lyapunov functions, the control \mathbf{u} is guaranteed to be globally stabilizing. In order to prove asymptotic stability, a theorem derived by Mukherjee and Chen¹⁴ is employed for the autonomous closed-loop equations. The theorem requires n more time derivatives of the Lyapunov function evaluated on the nonempty set of state vectors, Ω , satisfying $\dot{V}(\Omega) = 0$. If the first nonzero derivative evaluated on Ω is an odd numbered derivative (the third derivative, for example) and negative definite, then the system is asymptotically stable.

Starting from equation (21), the second time derivative of both Lyapunov functions is

$$\ddot{V}(\delta\boldsymbol{\omega} = 0, \boldsymbol{\eta}) = -2\delta\boldsymbol{\omega}^T [P] \delta\dot{\boldsymbol{\omega}} \quad (30)$$

Note that $\ddot{V} = 0$ in equation (30) because it is only a function of $\delta\boldsymbol{\omega}$, and $\delta\boldsymbol{\omega}$ goes to zero as time goes to infinity because the control is globally stabilizing. Evaluating the third time derivative yields:

$$\ddot{\ddot{V}}(\delta\boldsymbol{\omega} = 0, \boldsymbol{\eta}) = -2\delta\boldsymbol{\omega}^T [P] \delta\ddot{\boldsymbol{\omega}} - 2\delta\dot{\boldsymbol{\omega}}^T [P] \delta\dot{\boldsymbol{\omega}} \quad (31)$$

The first term goes to zero because it is a function of $\delta\boldsymbol{\omega}$. The next step is to solve the closed loop dynamics for $\dot{\boldsymbol{\omega}}$ and substitute into equation (31). Because the closed loop dynamics differ for the two Lyapunov functions, each must be analyzed separately. Substituting the closed-loop dynamics of the quadratic Lyapunov function into equation (31) yields:

$$\ddot{\ddot{V}}(\delta\boldsymbol{\omega} = 0, \boldsymbol{\eta}) = -2 \left[-[I]^{-1} [K] (1 + \eta^2) \frac{\Sigma_2 + a}{\Sigma_2} \boldsymbol{\eta} \right]^T [P] \left[-[I]^{-1} [K] (1 + \eta^2) \frac{\Sigma_2 + a}{\Sigma_2} \boldsymbol{\eta} \right] \quad (32)$$

The scalar values can be pulled to the front and the transpose operator distributed to produce the following result:

$$\ddot{V}(\delta\boldsymbol{\omega} = 0, \boldsymbol{\eta}) = -2 \left[[K] (1 + \eta^2) \frac{\Sigma_2 + a}{\Sigma_2} \right]^2 \boldsymbol{\eta}^T [I]^{-1} [P] [I]^{-1} \boldsymbol{\eta} \quad (33)$$

Because $[P]$ and $[I]$ are symmetric, positive definite, and $\Sigma_2 > 0$ for $a \neq 1$, the equation is quadratic in $\boldsymbol{\eta}$ and therefore negative definite. The Mukherjee and Chen Theorem is satisfied, so the control torque in equation (25) is asymptotically stabilizing for both states, $\delta\boldsymbol{\omega}$ and $\boldsymbol{\eta}$.

Following the same procedure for the logarithmic Lyapunov function provides the following result:

$$\ddot{V}(\delta\boldsymbol{\omega} = 0, \boldsymbol{\eta}) = -2 \left(K \frac{\Sigma_2 + a}{\Sigma_2} \right)^2 \boldsymbol{\eta}^T [I]^{-1} [P] [I]^{-1} \boldsymbol{\eta} \quad (34)$$

Again, the equation is quadratic in $\boldsymbol{\eta}$ and therefore negative definite. The Mukherjee and Chen Theorem is satisfied for both control laws and the states, $\delta\boldsymbol{\omega}$ and $\boldsymbol{\eta}$, will asymptotically converge to zero.

3.3 Linear Feedback Gain Selection

Proper feedback gain values must be selected before the control law derived in the previous section can be simulated. The intuitive MRP gain selection technique in Reference 5 in terms of desired linear damping ratios and damped frequency is expanded in this section to account for arbitrary projection points a .

First, the following combined state error vector $\boldsymbol{x} = [\boldsymbol{\eta} \ \delta\boldsymbol{\omega}]^T$ is introduced. The autonomous closed-loop dynamics in equation (22) are put into the following state space form:

$$\dot{\boldsymbol{x}} = \begin{Bmatrix} \dot{\boldsymbol{\eta}} \\ \delta\dot{\boldsymbol{\omega}} \end{Bmatrix} = \begin{bmatrix} 0 & \frac{1}{2} [D(\boldsymbol{\eta})] \\ -[I]^{-1} [K] (1 + \eta^2) \frac{\Sigma_2 + a}{\Sigma_2} & -[I]^{-1} [P] \end{bmatrix} \begin{Bmatrix} \boldsymbol{\eta} \\ \delta\boldsymbol{\omega} \end{Bmatrix} \quad (35)$$

To simplify these equations further for linear analysis, $[I]$, $[P]$, and $[K]$ are assumed to be diagonal matrices with positive entrees. This assumption allows the linear closed-loop dynamics to be decoupled as follows:

$$\begin{Bmatrix} \dot{\eta}_i \\ \delta\dot{\omega}_i \end{Bmatrix} = \underbrace{\begin{bmatrix} 0 & \frac{1}{2} \frac{1}{1-a} \\ -\frac{K_i}{I_i(1-a)} & -\frac{P_i}{I_i} \end{bmatrix}}_{[A]} \begin{Bmatrix} \eta_i \\ \delta\omega_i \end{Bmatrix} \quad (36)$$

where $i = \{1, 2, 3\}$.

With the logarithmic Lyapunov function, the linearization of equation (28) is essentially identical to equation (36). The only exception is the condition that $K_1 = K_2 = K_3$ because the gain for the logarithmic Lyapunov function is a scalar.

A linear analysis can now be preformed by calculating the characteristic equation of the linearized state matrix $[A]$:

$$\lambda^2 + \frac{P_i}{I_i} \lambda + \frac{K_i}{2I_i(1-a)^2} = 0 \quad (37)$$

Equation (37) can be compared to the characteristic equation for a general damped second order system, given as $\lambda^2 + 2\zeta\omega_n\lambda + \omega_n^2 = 0$. Comparing the two equations, the natural frequency and damping ratio are solved for as:

$$\omega_{n,i} = \sqrt{\frac{K_i}{2I_i(1-a)^2}} \quad (38)$$

$$\zeta_i = \frac{P_i |1 - a|}{\sqrt{2K_i I_i}} \quad (39)$$

An intuitive way to select the linear feedback gains is by choosing the decay time constant and the damped natural frequency, both of which have physical meaning to the system. The decay time constant, T_i , indicates how long it would take for the state errors to decay to $1/e$ of their respective initial values, and is given by:

$$T_i = \frac{1}{\zeta_i \omega_{n,i}} = \frac{2I_i}{P_i} \quad (40)$$

It is interesting to note that the angular velocity feedback gains P_i determine how fast the state errors will decay. The attitude feedback gains K_i only affect the damped natural frequency of the closed loop system, given by:

$$\omega_{d,i} = \omega_{n,i} \sqrt{1 - \zeta_i^2} = \frac{1}{2I_i} \sqrt{2 \frac{K_i I_i}{(1 - a)^2} - P_i^2} \quad (41)$$

The performance can now be specified for each mode of the linear system in terms of the $(\omega_{d,i}, T_i)$ characteristics for the closed loop system. Specifying these quantities allows $[K]$ (or scalar K) and $[P]$ to be chosen. The resulting gain matrices are used in the nonlinear system, although the performance will not in general be identical to that predicted by the linear analysis. The control law combined with this method of gain selection is examined in the next section. Note that with the projection point $a = -1$ the MRP gain selection technique in Reference 5 is regained.

4 Numerical Simulation

The following simulations illustrate a scenario where the desired singularity is at $\hat{\Phi} = 30^\circ$, which results in a projection point $a = 0.9659$. These simulations track a fixed direction and force the angular velocities to zero, therefore the reference angular velocity in equation (29) is zero. The initial SSOP values are chosen to be close to the singularity to explore an extreme scenario that the control law may encounter during operation. The inertia matrix is chosen to be $[I] = \text{diag}[250 \ 200 \ 180] \text{kg} \cdot \text{m}^2$. A fourth order Runge-Kutta integrator is used in these simulations with a time step of 0.05 seconds.

The feedback gains are chosen using the linear analysis presented in the previous section. In order to compare the results of the quadratic and logarithmic Lyapunov functions, the diagonal elements of $[K]$ are set equal to the scalar K . By choosing the time decay values to be $T = [2.5 \ 1.5 \ 6]^T$ seconds, the values of $[P]$ can be solved for using equation (40) which yields $[P] = \text{diag}[200 \ 266.67 \ 60] \text{kgm}^2/\text{s}$. The value of K can be found by solving equation (39) yielding:

$$K_i = \frac{P_i^2 (1 - a)^2}{2I_i \zeta_i^2}$$

The value of ζ_i is now chosen to calculate a value for K_i . The first mode is chosen to be critically damped (i.e. $\zeta_1 = 1$) with $K_1 = 0.0929 \text{ kg} \cdot \text{m}^2/\text{s}^2$. For comparison, the other two diagonal terms of $[K]$ are set equal to K_1 . It is useful to see the damping ratio for the other two modes which turns out to be $\zeta_2 = 1.4907$ and $\zeta_3 = 0.3536$. Therefore the second mode is expected to be over-damped in the end game, and the third mode is expected to be under-damped.

The initial SSOP is set to $\boldsymbol{\eta} = [8.1597 \ 1.7532 \ 25.2985]^T$ which corresponds to a principal angle of $\Phi_0 = 26^\circ$. It is chosen to be close to the desired singularity point at $\hat{\Phi} = 30^\circ$ to provide the control law with a worst case scenario. In this spirit, the angular velocities are chosen to push the spacecraft towards the singularity with values of $\boldsymbol{\omega} = [0.1 \ -0.05 \ 0.05]^T \text{rad/s}$.

The SSOPs for the resulting reorientation maneuver are shown in Fig. 3. The orientation is pushed away from the desired direction initially by the initial angular velocities and peak at about

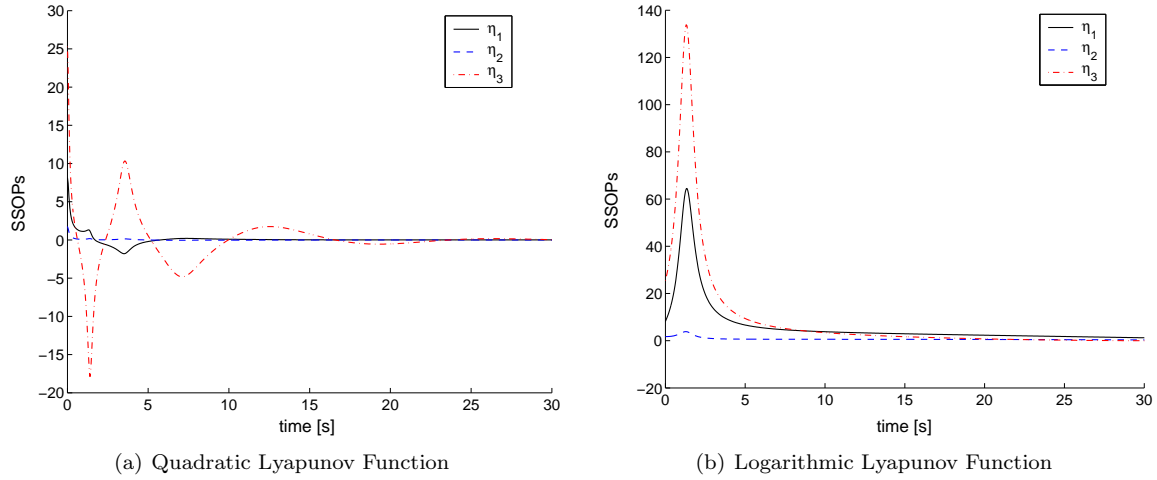


Figure 3. Symmetric Stereographic Orientation Parameters

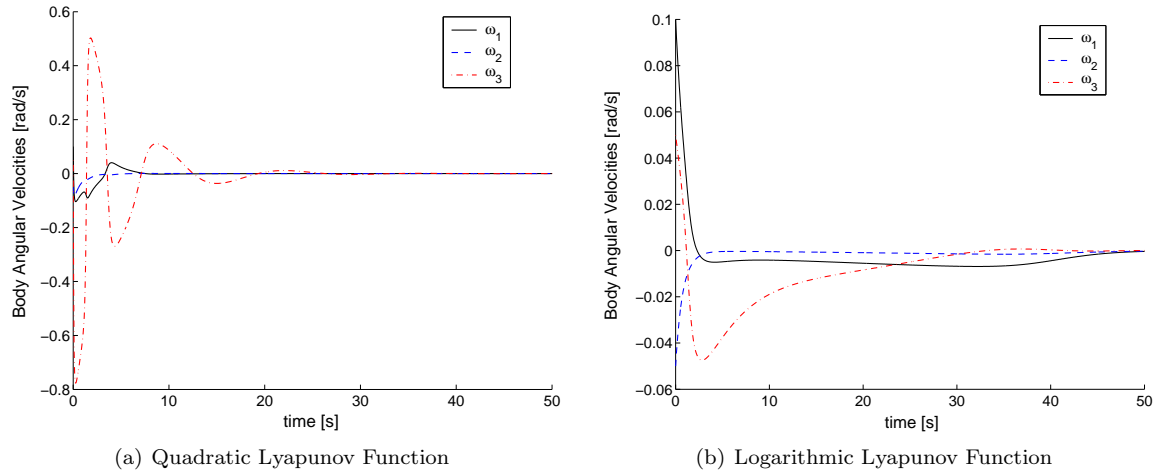


Figure 4. Body Angular Velocities

one second. The control torques then bring the values back to the desired fixed orientation. The SSOPs for the logarithmic function grow much larger and thus get closer to the singularity. However, this logarithm-based control makes a much smoother transition than the quadratic-based control as it converges to the fixed orientation. Notice the quadratic Lyapunov function tends to be much more aggressive with large attitude errors and causes the SSOPs to oscillate about the fixed direction.

The control torques cause the angular velocities, shown in Fig. 4, to grow larger in order to rotate the craft to the desired direction. The angular velocities then decay back to zero. The angular velocities associated with the quadratic Lyapunov function return to zero quickly whereas the logarithmic function slowly approaches zero. The logarithmic function appears to try and ease the spacecraft into position whereas the quadratic function wants to slam it into place.

This aggressive behavior of the quadratic-based control with near-singular orientations is also apparent in the control torques shown in Fig. 5. For the quadratic function, the torque magnitudes reach over 1000 N·m which is fifty times the greatest control torque used in the logarithmic case. The quadratic function also tends to create spikes in the control torques which causes jerky motion in the spacecraft. These jerky motions are obvious in the graph of principal rotation angles shown in Fig. 6.

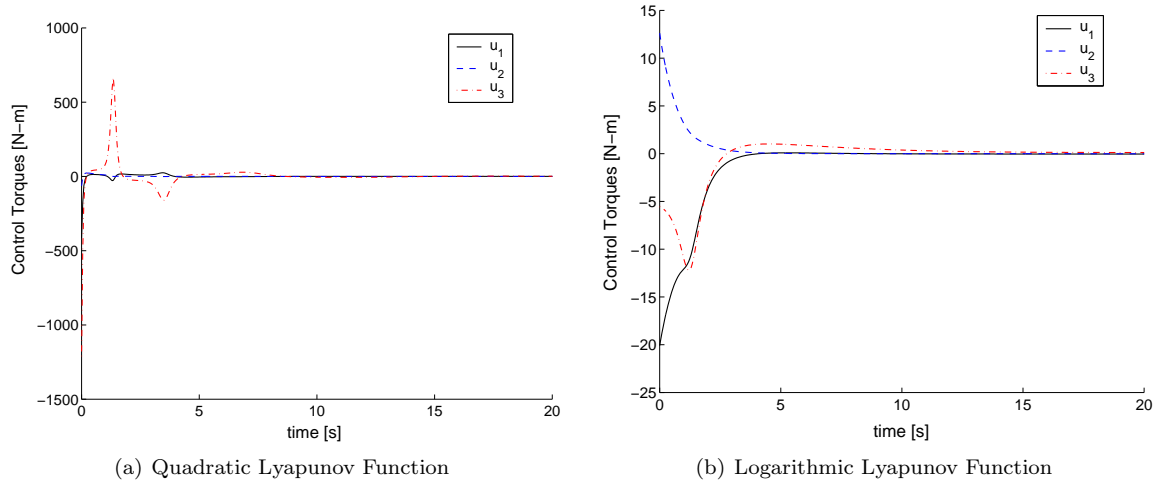


Figure 5. Control Torques

The trade off is time it takes for the spacecraft to reach the fixed direction which is about 50 seconds for the logarithmic function and 30 seconds for the quadratic. However, note that the quadratic control's feedback gain matrix $[K]$ values can be set independently for each body axis to have all modes critically damped. This would change the transient response somewhat. This simulation is set up such that both quadratic- and logarithmic-based controls have the same linear closed loop response in the end game. This provides a better illustration of how the logarithmic-based control provides better performance with large attitude errors, while the quadratic-based control becomes overly aggressive.

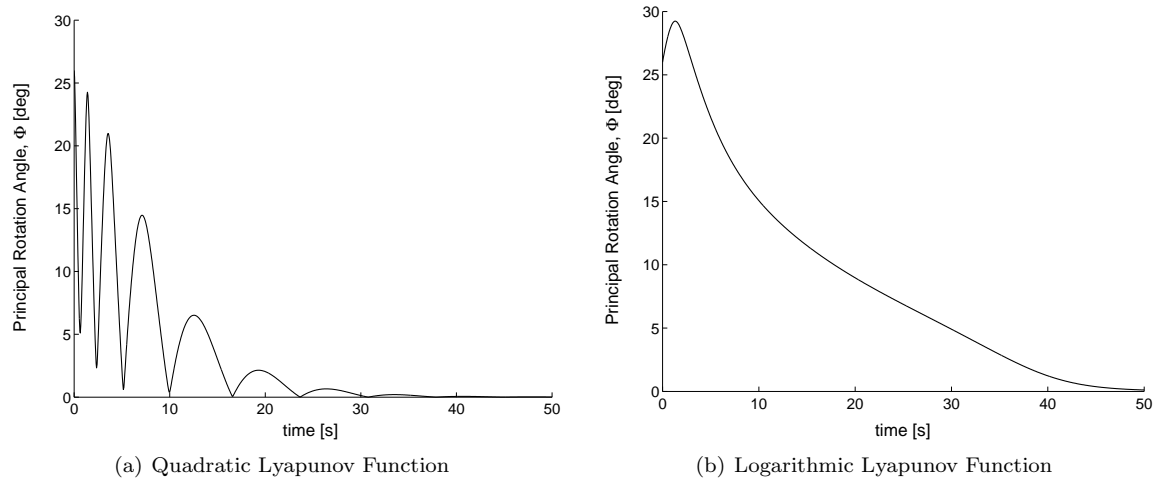


Figure 6. Principal Rotation Angle

Once the SSOP values become sufficiently small, the nonlinear end game behavior mirrors the linear response. This illustrates that both the quadratic- and logarithmic-based control strategies exhibit the expected linear end game response with the chosen feedback gains. Note that this simulation uses a worst case scenario where the orientation is rapidly approaching a singular orientation. If $\Phi < \hat{\Phi}/2$ during the maneuver, then the logarithmic-based control provides an essentially linear response. This has been illustrated earlier in Reference [5] where the MRP attitude control law has a $\hat{\Phi} = 360$ degrees and errors as large as 180 degrees still result in near-linear closed-loop dynamics.

The results in this paper generalize this control for arbitrary $\hat{\Phi}$ singular orientations.

5 Conclusion

This paper fully develops the symmetric stereographic orientation parameters by parameterizing the direction cosine matrix in terms of the SSOPs, deriving the kinematic differential equations for any projection point, and discussing SSOP uniqueness issues if $\hat{\Phi}$ is not 180° or 360° . The SSOPs allow the singular principal rotation angle of the attitude representation to be chosen at will. This allows a simple feedback control law to be designed that constrains the attitude motion between the singular configurations. Therefore the singular configurations can be placed at particular orientations that the rigid body must never exceed and bound the attitude motion within a desired range. The design and implementation of such a control law for a simple spacecraft system is presented as well as a simple approach for gain selection using linear theory. This control generalizes previously developed CRP and MRP based attitude control laws for any SSOP projection point and associated singularity. Numerical simulations show that the control law successfully regulates the spacecraft about the desired attitude. Even for large initial angular velocities the attitude is bounded within a specific range. Future work will consider how to incorporate torque saturation issues into this development where the singular boundaries may be penetrated.

References

- [1] SCHAUB, H. and JUNKINS, J. L., *Analytical Mechanics of Space Systems*, AIAA Education Series, Reston, VA, 1st edn., 2003.
- [2] MARANDI, S. R. and MODI, V. J., "A Preferred Coordinate System and the Associated Orientation Representation in Attitude Dynamics", *Acta Astronautica*, Vol. 15, No. 11, 1987, pp. 833–843.
- [3] SHUSTER, M. D., "A Survey of Attitude Representations", *Journal of the Astronautical Sciences*, Vol. 41, No. 4, 1993, pp. 439–517.
- [4] TSIOTRAS, P., "New Control Laws for the Attitude Stabilization of Rigid Bodies", *13th IFAC Symposium on Automatic Control in Aerospace*, Palo Alto, CA, Sept. 12–16 1994, (pp. 316–321).
- [5] SCHAUB, H. and JUNKINS, J. L., "Stereographic Orientation Parameters for Attitude Dynamics: A Generalization of the Rodrigues Parameters", *Journal of the Astronautical Sciences*, Vol. 44, No. 1, Jan.–Mar 1996, pp. 1–19.
- [6] AKELLA, M. R., "Rigid Body Attitude Tracking Without Angular Velocity Feedback", *Systems and Control Letters*, Vol. 42, 2001, pp. 321–326.
- [7] SPINDLER, K., "Attitude Maneuvers which Avoid a Forbidden Direction", *Journal of Dynamical and Control Systems*, Vol. 8, Jan 2002, pp. 1–22.
- [8] TSIOTRAS, P., "A Passivity Approach to Attitude Stabilization Using Nonredundant Kinematic Parameterizations", *34th IEEE Conference on Decision and Control*, Dec. 13–15, 1995, pp. 515–520.
- [9] ROBINETT, R. D., PARKER, G. G., SCHAUB, H., ET AL., "Lyapunov Optimal Saturated Control for Nonlinear Systems", *AIAA Journal of Guidance, Control, and Dynamics*, Vol. 20, No. 6, Nov.–Dec. 1997, pp. 1083–1088.
- [10] WALLSGROVE, R. J. and AKELLA, M. R., "Globally Stabilizing Saturated Attitude Control in the Presence of Bounded Unknown Disturbances", *AIAA Journal of Guidance, Control, and Dynamics*, Vol. 28, No. 5, 2005, pp. 957–963.
- [11] TSIOTRAS, P., "New Control Laws for the Attitude Stabilization of Rigid Bodies", *IFAC Symposium on Automatic Control in Aerospace*, Sept. 12–16, 1994, pp. 833–843.
- [12] MARANDI, S. R. and MODI, V. J., "A Preferred Coordinate System and the Associated Orientation Representation in Attitude Dynamics", *Acta Astronautica*, Vol. 15, 1987, pp. 833–843.
- [13] STANLEY, W. S., "Quaternion from Rotation Matrix", *Journal of Guidance and Control*, Vol. I, No. 3, 1978, pp. 223–224.
- [14] MUKHERJEE, R. and CHEN, D., "Asymptotic Stability Theorem for Autonomous Systems", *Journal of Guidance, Control, and Dynamics*, Vol. 16, Sept.–Oct. 1993, pp. 961–963.

- [15] CRAIG, R. R., JR., *Structural Dynamics: An Introduction to Computer Methods*, John Wiley & Sons, New York, NY, 1st edn., 1981.